Electromagnetic Field Analysis and Calculation of the Resonance Characteristics of the Loop-Gap Resonator

MEHRDAD MEHDIZADEH, MEMBER, IEEE, AND T. KORYU ISHII, SENIOR MEMBER, IEEE

Abstract —**The electromagnetic field configuration of the loop-gap resonator is analyzed and expressions for field distributions are derived. The method involves solving Maxwell's equations for the boundary conditions and matching the internal magnetic fields of the resonator to the evanescent fringing fields by a numerical fitting method. The expressions derived from this analysis are used in the derivation of equations for the resonant frequency and the quality factor of the resonator. The computed results are in good agreement with the measured values for resonant frequency and quality factors.**

I. Introduction

THE CHARACTERISTICS and applications of the loop-gap resonator have been discussed in a number of recent publications [1]–[3]. Attempts to elaborate a field analysis and derive equations for the resonant frequency and the quality factor of this type of resonator were made in [1] and [2]. In the simple analysis in [1], where the fringing fields are not considered, the equation derived on the basis of this model gives only a rough estimate of the resonant frequency compared to measured results. In [2], the addition of an empirical factor for the fringing capacitance of the gap gives better accuracy. In [3] expressions for the resonant frequency and quality factor are presented, where empirical factors for fringing fields are given. The purpose of this paper is to theoretically treat the problem considering both electric and magnetic fringing fields and to derive more accurate equations for the resonant frequency and the quality factor based on this analysis.

Fig. 1 shows the electromagnetic field configuration and the direction of surface currents for a loop-gap resonator. The electric fields are supported between the two parallel surfaces of the gap, and the magnetic fields surround the loop; thus the conduction current flows circumferentially on the surfaces of the resonator and the shield. The magnetic field intensity in the central region and also in the annular region can be considered to be uniform for small gap distances. The magnetic fields which are located within the length of the resonator are termed main magnetic fields in this paper; the curved magnetic field lines which are located outside of the resonator length and connect the field lines of the central and annular regions are called fringing magnetic fields.

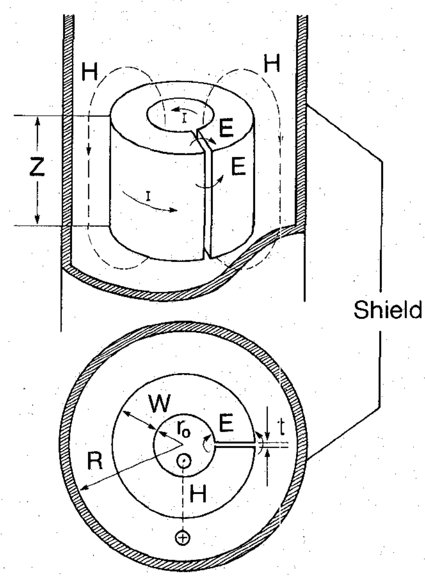

Fig. 1. The electromagnetic field configuration and direction of currents in a loop-gap resonator.

As shown in Fig. 1, a loop-gap resonator is considered in this paper with an inner loop radius r_0, a gap distance t, a gap width W, and a length Z. The resonator is coaxial with a shield of radius R and a length much larger than Z.

In Section II the magnetic fringing fields are analyzed. An equation for the overall balance of electric and magnetic stored energies is derived in Section III which leads to the derivation of an equation for the resonant frequency. In Section IV the developed field distribution theory is used for the derivation of an expression for the

Manuscript received September 8, 1988; revised February 13, 1989. This work was supported in part by Grants RR1008 and GM7665 from the National Institute of Health.

M. Mehdizadeh was with the Department of Electrical Engineering and Computer Science, Marquette University, and with the National Biomedical ESR Center, the Medical College of Wisconsin, He is now with the NMR Science and Technology Center, Picker International Inc., Highland Heights, OH 44143.

T. K. Ishii is with the Department of Electrical Engineering and Computer Science, Marquette University, Milwaukee, WI 53233.

IEEE Log Number 8927840.

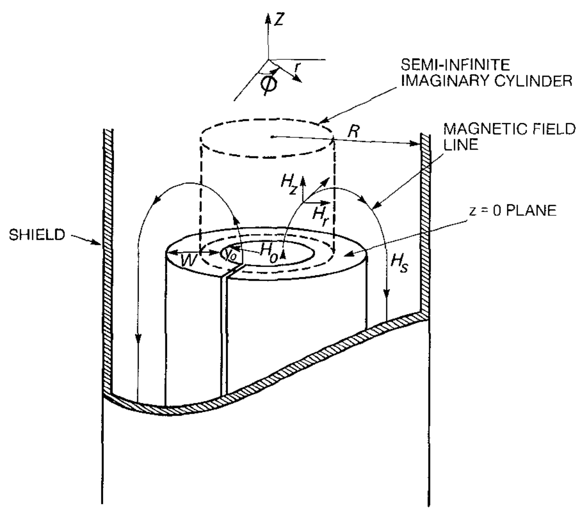

Fig. 2. Fringing magnetic field configuration on one end of a loop-gap resonator.

quality factor, and in Section V a comparison of calculated and measured results is presented.

II. Analysis of Magnetic Field Distribution

A detailed view of magnetic fields at one end of a loop-gap resonator is shown in Fig. 2, where a cylindrical coordinate system (r, ϕ, z) is considered where the origin of the z coordinate is on the top surface plane of the resonator. For $z \leqslant 0$, the magnetic field intensities H_0 and $-H_S$ are defined for the central and the annular region of the resonator as shown. These fields, which are approximated to be uniform, are defined as main magnetic fields. For $z > 0$ the curved fringing fields are considered to have components H_r and H_z, neglecting the angular asymmetry because of the gap.

In a typical resonator the shield radius is much smaller than the resonant wavelength; so the fields at $z > 0$ can be represented by a summation of evanescent cylindrical TE_{0n} modes within the shield [4], [5]:

$$H_z(r,z) = \sum_{n=1}^{\infty} H_{0n} J_0\left(\frac{U'_{01}}{R} r\right) e^{-a_{0n} z} \tag{1}$$

$$H_r(r,z) = \sum_{n=1}^{\infty} H_{0n} \frac{a_{0n} R}{U'_{0n}} J'_0\left(\frac{U'_{01}}{R} r\right) e^{-a_{0n} z}. \tag{2}$$

Here J_0 is the Bessel function of first kind and order zero, H_{0n} and a_{0n} are the amplitude and the attenuation constant of the nth mode, respectively, and U'_{0n} is the root of $J'_0(x) = 0$. Then

$$a_{0n} = \frac{2\pi}{\lambda}\sqrt{\left(\frac{\lambda}{\lambda_{con}}\right)^2 - 1}\,. \tag{3}$$

The parameter λ is the resonance wavelength and λ_{con} is the cutoff wavelength of the nth mode, given by

$$\lambda_{con} = \frac{2\pi R}{U_{0n}}.$$

Considering the first mode, TE_{01}, as dominant, the effect of all other modes is taken into account by the two continuous functions $\xi_1(r)$ and $\xi_2(r)$ as factors of the z-directed and r-directed components of this mode respectively:

$$H_z(r,z) = H_0 J_0(Kr) \xi_1(r) e^{-a_{01} z} \tag{4}$$

$$H_r(r,z) = H_0 \frac{a_{01}}{K} J_1(Kr) \xi_2(r) e^{-a_{01} z}. \tag{5}$$

To determine $\xi_1(r)$ and $\xi_2(r)$, consider the boundary conditions on the field components. First, as shown in Fig. 2, the magnetic field intensity at the plane $z = 0$ is only z-directed:

$$H_r(r,0) = 0. \tag{6}$$

Second, H_z at the center of the $z = 0$ plane is equal to the magnetic field intensity at the central region:

$$H_z(0,0) = H_0. \tag{7}$$

Third, the magnetic fluxes passing through the following surfaces should be equal: the cross section of the central region, the semi-infinite cylindrical imaginary surface S as shown in Fig. 2, and the annular region cross section, or

$$\int_0^{2\pi}\int_0^{r_0} H_z(r,0)\, r\, dr\, d\phi$$
$$= \int_0^{\infty}\int_0^{2\pi}\left(r_0 + \frac{W}{2}\right) H_r\left(r_0 + \frac{W}{2}, z\right) d\phi\, dz$$
$$= \int_0^{2\pi}\int_{r_0+W}^{R} r H_z(r,0)\, dr\, d\phi. \tag{8}$$

In addition to the above boundary conditions the magnetic field vector function should follow Maxwell's divergence equation:

$$\nabla \cdot \boldsymbol{H} = 0. \tag{9}$$

Inserting (3) and (4) into the above divergence equation yields

$$\frac{d\xi_1}{dr} = K\frac{J_0(Kr)}{J_1(Kr)}\left[\xi_1(r) - \xi_2(r)\right]. \tag{10}$$

Since the functions ξ_1 and ξ_2 are continuous and well behaved, a polynomial of order 3 was chosen for ξ_1, and the coefficients of this polynomial can be found from boundary conditions (6) and (7), and (8). Then the function ξ_2 was evaluated by solving the differential equation (10) using a numerical method.

III. Resonant Frequency of the Loop-Gap Resonator

In the following analysis the effects of magnetic fringing fields are taken into account by considering uniform magnetic fields over a length $Z + \Delta Z$, where Z is the physical length of the resonator and ΔZ is an equivalent length extension due to the magnetic fringing fields. Similarly, the effects of the fringing electric fields in the gap area are accounted for by considering uniform electric fields over a gap width of $W + \Delta W$, where W is the physical width of the gap and ΔW is an equivalent gap width extension due

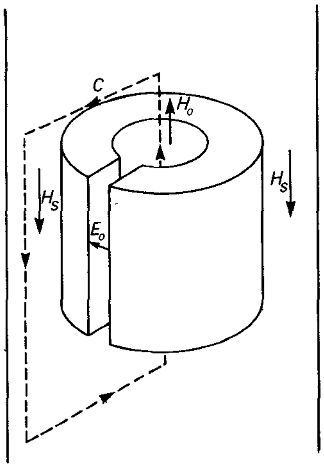

Fig. 3. Integral contour for application of Ampere's law on the gap.

to the electric fringing fields. Expressions for ΔZ and ΔW will be derived later in this section.

With the above considerations, application of Ampere's law on the closed contour C in Fig. 3 yields

$$(Z+\Delta Z)(H_0+H_S)=j\omega_0\epsilon_0 E_0(W+\Delta W)Z \quad (11)$$

where ω_0 is the angular frequency and H_0 and H_S are the magnetic field intensities of the central and annular regions, respectively. It should be noted that the radially directed segment of contour C in the evanescent region and the magnetic field along these segments are considered to be zero. Applying the equivalence of electric and magnetic stored energies at resonance gives

$$\frac{1}{2}\epsilon_0\iiint_{V_g} E_0^2\,dv=\frac{1}{2}\mu_0\iiint_{V_c} H_0^2\,dv+\frac{1}{2}\mu_0\iiint_{V_a} H_s^2\,dv \quad (12)$$

where V_g is the volume in the gap, V_c is the volume of the central region, and V_a is the volume of the annular region.

Because of small skin depth, the energy stored in conductors is neglected. Expansion of (12) gives

$$\frac{1}{2}\mu_0 H_0^2\pi r_0^2(Z+\Delta Z)+\frac{1}{2}\mu_0 H_S^2\pi\left[R^2-(r_0+W)^2\right]\cdot(Z+\Delta Z)=\frac{1}{2}\epsilon_0 E_0^2(W+\Delta W)tZ. \quad (13)$$

The fringing field energy at the gap at both ends of the cylinder is neglected because most of the energy is confined within the gap along the z direction.

The equivalence of magnetic fluxes over the central region and the annular region cross sections is expressed in (8); expansion of the first and third parts of this equation yields

$$H_S=\frac{r_0^2}{R^2-(r_0+W)^2}H_0. \quad (14)$$

Combining (1), (13), and (14), an expression for the resonant frequency is obtained:

$$f_0=\frac{v}{2\pi r_0}\sqrt{\frac{t}{\pi W}}\sqrt{1+\frac{r_0^2}{R^2-(r_0+W)^2}}\sqrt{\frac{1+\dfrac{\Delta Z}{Z}}{1+\dfrac{\Delta W}{W}}} \quad (15)$$

where v is the velocity of light in free space.

A. Calculation of ΔZ

The magnetic energy stored in both the central and the annular region of the resonator with uniform fields and the length of ΔZ can be found using equation (14):

$$W_f=\frac{1}{2}\mu_0\pi r_0^2H_0^2\left(1+\frac{r_0^2}{R^2-(r_0+W)^2}\right)\Delta Z. \quad (16)$$

The stored magnetic fringing field energies in the z and r directions, W_{H_z} and W_{H_r}, are determined from the field distribution equations (3) and (4) to be

$$W_{H_z}=\frac{1}{2}\mu_0\pi H_0^2\frac{1}{a_{01}}\int_0^R rJ_0^2(Kr)\xi_1^2(r)\,dr \quad (17)$$

$$W_{H_r}=\frac{1}{2}\mu_0\pi H_0^2\frac{a_{01}}{K^2}\int_0^R rJ_1^2(Kr)\xi_2^2(r)\,dr. \quad (18)$$

The total magnetic fringing field energy at both ends of the resonator is

$$W_f=2(W_{H_z}+W_{H_r}). \quad (19)$$

Combining (16), (17), and (19) gives

$$\Delta Z=\frac{2\left[\int_0^R rJ_0(Kr)\xi_1^2(r)\,dr+\left(\frac{a_{01}}{K}\right)^2\int_0^R rJ_1(Kr)\xi_2^2(r)\,dr\right]}{r_0^2(1+\rho)a_{01}}. \quad (20)$$

B. Calculation of ΔW

Consider the gap as a lumped capacitor (Fig. 4(a)) which consists of a uniform parallel plate and a fringing capacitance. From the definition of ΔW above, the fringing capacitance, C_f, is

$$C_f=\frac{\epsilon_0\Delta WZ}{t}. \quad (21)$$

The curved shape of this capacitor can be transformed into the simpler coplanar capacitor shape of Fig. 4(b) by a conformal transformation [6]:

$$w=\ln z \quad (22)$$

where z and w are complex planes associated with Fig. 4(a) and 4(b), respectively. The total fringing capacitance

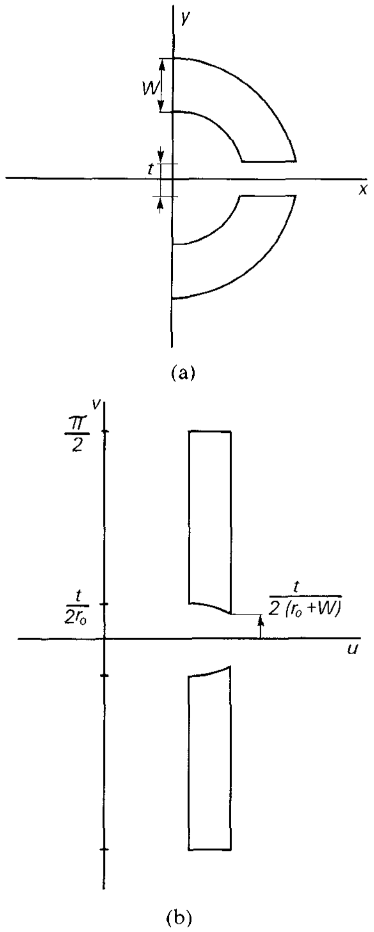

Fig. 4. Conformal mapping of the gap area cross section: (a) plane $x-y$; (b) plane $U-V$

is then [7]

$$C_f = \frac{\epsilon_0}{2}\left(\frac{K\left(\sqrt{1-k_t^2}\right)}{K(k_t)} + \frac{K\left(\sqrt{1-k_0^2}\right)}{K(k_0)}\right)Z \tag{23}$$

where

$$K_t = \frac{t}{\pi r_0} \qquad K_0 = \frac{t}{\pi(r_0+W)} \tag{24}$$

and K is the complete elliptic integral. Combining (23) and (21) gives

$$\Delta W = \frac{t}{2}\left(\frac{K\left(\sqrt{1-k_t^2}\right)}{K(k_t)} + \frac{K\left(\sqrt{1-k_0^2}\right)}{K(k_0)}\right). \tag{25}$$

IV. Quality Factor of the Loop-Gap Resonator

Power loss on the conductor surfaces of a resonator is generally given by [8]

$$P_L = \frac{1}{2\sigma\delta_s}\int_S\int |H_{\tan}|^2\, ds \tag{26}$$

where $H_{\tan}$ is the tangential component of the magnetic field intensity on the surfaces, σ is the surface conductivity, and δ_s is the skin depth. Considering the magnetic field distribution derived in Section II, the total ohmic losses on the surfaces of the resonator are formulated as follows:

$$P_L = \frac{1}{2\sigma\delta_s}\left[\int_0^Z\int_0^{2\pi} r_0 H_0^2\, d\phi\, dz + \int_0^Z\int_0^{2\pi}(r_0+W)H_S^2\, d\phi\, dz + \int_0^Z\int_0^{2\pi} R H_S^2\, d\phi\, dz + 2\int_Z^\infty\int_0^{2\pi} R H_Z|_{r=R}^2\, d\phi\, dz\right]. \tag{27}$$

In the above equation the first term represents losses on the inner wall of the loop, the second term for the outer wall of the loop. The third term shows losses on the inner wall of the shield, and the fourth term corresponds to the losses due to fringing magnetic fields on the inner wall of the shield. The ohmic losses at both end surfaces of the loop are neglected.

The energy stored in the resonator, W_S, is given by either side of (13); then the quality factor considering only ohmic losses on the cylindrical walls of the resonator, Q_S, is

$$Q_S = \frac{\omega_0 W_S}{P_L}. \tag{28}$$

Expanding (27) for losses and inserting into (28) gives

$$Q_S = \frac{r_0}{\delta}\,\frac{(1+\rho)\left(1+\dfrac{\Delta Z}{Z}\right)}{1+\left(1+\dfrac{W}{r_0}+\dfrac{R}{r_0}+\dfrac{R^2}{U_{01}'Zr_0}\right)\rho^2} \tag{29}$$

where

$$\rho = \frac{r_0^2}{R^2-(r_0+W)^2}. \tag{30}$$

If the length of the resonator, Z, is set to infinity, (28) will reduce to the length-independent equation given in [1]. In the above derivations, the ohmic losses in the gap (capacitor losses) are not considered; therefore quality factors calculated by (29) are considerably higher than the measured results. An expression for calculation of ohmic losses in a parallel-plate capacitor is given in [9]. Modification of this equation for the loop-gap resonator geometry [2] gives the following equation for the gap quality factor:

$$Q_C = \frac{1.7\times10^5 t}{f^{3/2}\epsilon_0 W^2\left(1+\dfrac{\Delta W}{W}\right)}. \tag{31}$$

The overall unloaded quality factor, Q_0, can be found using (29) and (31):

$$\frac{1}{Q_0} = \frac{1}{Q_S} + \frac{1}{Q_C}. \tag{32}$$

TABLE I
COMPARISON OF THE RESULTS OF THEORETICAL CALCULATIONS AND EXPERIMENTAL MEASUREMENTS FOR VARIOUS LOOP-GAP RESONATORS

Res. #	r_0	W	t	Z	R	MEAS. f_0 (MHz)	THEORY f_0(MHz)	MEAS. Q_0	THEORY Q_0
1	6.35	6.35	.254	15.02	30.50	1083.3	1048.4	1600	1910
2	6.35	2.54	.228	19.05	17.80	1381.8	1321.9	2100	2280
3	3.17	6.35	.280	19.05	30.22	2222.1	2207.0	1360	1423
4	3.17	6.35	.280	10.20	36.60	2817.2	2855.8	1725	1850
5	2.36	2.34	.254	9.52	11.0	3690.0	3641.2	1680	1724
6	1.50	.80	.330	3.98	5.08	8877.9	9163.9	725	790
7	1.09	1.27	.330	3.98	5.08	10356.2	10756.2	556	605

All dimensions are in millimeters.

V. THEORETICAL VERSUS EXPERIMENTAL RESULTS

Calculations of the resonant frequency and the quality factor for a given resonator were performed by numerical calculations of ΔZ and ΔW using (20) and (25) and substitution of the result into (15) for the resonant frequency and into (29) and (31) for the quality factor. Table I shows results of calculations and measurements for seven resonators with resonant frequencies ranging from 1 to 10 GHz. It should be noted that the resonant frequency is very sensitive to the gap distance; therefore limitations on precision of manufacturing and measurement of the gap distance create an uncertainty in the comparison of measured and calculated values, which in the case of this work can be as high as 3 percent.

VI. CONCLUSIONS

A method for the electromagnetic field analysis of a loop-gap resonator was developed where both electric and magnetic fringing fields are taken into account. For magnetic fields, the TE evanescent modes are matched to the internal fields of the resonator by a numerical fitting method, and for electric fields, the conformal mapping method is used. The results of this field analysis were used in deriving equations for the resonant frequency and the quality factor. Good agreement between theoretical and experimental results was obtained.

VII. DISCUSSION

1) To the authors' knowledge, no exact solution of the electromagnetic fields of the loop-gap resonator exists to date. Therefore approximate solutions [1] and [2] were used as starting points of the analysis.

2) Due to geometrical constraints of the practical resonator, only the TE_{0n} mode used in this analysis is meaningful.

3) If the gap is large, the rotational symmetry is perturbed by the gap and the condition in (6) is affected. For the small-gap condition considered here, the perturbation effect is negligible.

4) The present analysis produces results which agree with measurements. An alternative theoretical approach involves using a suitable variational formula where the perturbation field due to the gap is approximated by a linear combination of known functions and the Rayleigh–Ritz method [10].

ACKNOWLEDGMENT

The authors would like to thank Dr. J. S. Hyde of the Medical College of Wisconsin for his encouragement and valuable discussions.

REFERENCES

[1] W. N. Hardy and L. A. Whitehead, "Split-ring resonator for use in magnetic resonance from 200–2000 MHz," *Rev. Sci. Instr.*, vol. 52, pp. 213–216, Feb. 1981.

[2] W. Froncisz and J. S. Hyde, "The loop-gap resonators: A new microwave lumped circuit ESR sample structure," *J. Magn. Resonance*, vol. 47, pp. 515–521, 1982.

[3] M. Mehdizadeh, T. K. Ishii, J. S. Hyde, and W. Froncisz, "Loop-gap resonator: A lumped mode microwave resonant structure for *L* and *S* bands," *IEEE Trans. Microwave Theory Tech.*, vol. MTT-31, pp. 1053–1061, Dec. 1983.

[4] T. K. Ishii, *Microwave Engineering*. New York: Ronald Press, 1966.

[5] M. Mehdizadeh, Ph.D. dissertation, Marquette University, Milwaukee, WI, 1983.

[6] K. J. Binns, *Analysis and Computation of Electric and Magnetic Field Problems*. New York: Pergamon Press, 1964, pp. 122–123.

[7] I. J. Bahl and R. Garg, *Microstrip Lines and Slot Lines*. Dedham, MA: Artech House, 1980, pp. 268–269.

[8] R. E. Collin, *Foundations for Microwave Engineering*. New York: McGraw-Hill, 1966, pp. 324–327.

[9] M. Caulton, "Lumped elements in microwave integrated circuits," *IEEE Trans. Microwave Theory Tech.*, pp. 713–721, Dec. 1967.

[10] R. E. Collin, *Field Theory of Guided Waves*. New York: McGraw-Hill, 1960.

✠

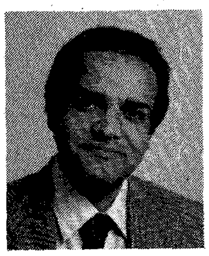

Mehrdad Mehdizadeh (S'79–M'83) received the B.S.E.E. degree from the Arya-Mehr University of Technology, Tehran, Iran, in 1977 and the M.S.E.E. and Ph.D. degrees in electrical engineering from Marquette University, Milwaukee, WI, in 1980 and 1983, respectively.

From 1981 to 1983 he performed research on lumped-mode microwave resonators in a joint project with the National Biomedical ESR Center, Medical College of Wisconsin, and the Department of Electrical Engineering at Marquette University. He worked in the microwave industry during 1984 and 1985. At General Microwave Corporation, Amityville, NY, he was engaged in the development of microwave system components, mainly new varactor-tuned microwave filter designs. Then he worked on microwave filters for K&L Microwave Inc., Salisbury, MD. In 1985 he joined NMR Science and Technology Division, Picker International, Highland Heights, OH, were he is engaged in research and development on RF probes and related subsystems for magnetic resonance imaging scanners.

Dr. Mehdizadeh holds two U.S. patents and has four patents pending. He is a member of Sigma Xi

Thomas Koryu Ishii (M'55–SM'65) was born in Tokyo, Japan on March 18, 1927. He received the B.S. degree in electrical engineering from Nihon University, Tokyo, in 1950 and the M.S. and Ph.D. degrees in 1957 and 1959, respectively, in electrical engineering from the University of Wisconsin, Madison. He also received the doctor of engineering degree from Nihon University in 1961.

From 1949 to 1956 he did research on microwave circuits and amplifiers and was an instructor at Nihon University. From 1956 to 1959 he did research on the noise figures of microwave amplifiers at the University of Wisconsin. Since 1959, he has been with Marquette University, Milwaukee, WI. At present he is a Professor of Electrical Engineering. The research areas include millimeter-wave and microwave ferrite devices, thermionic and solid-state devices, circuit components and transmission lines, and applications of microwaves, millimeter waves, and quantum electronics.

Dr. Ishii is a member of Sigma Xi, Eta Kappa Nu, Sigma Phi Delta, Tau Beta Pi, ASEE, AAUP, PCM, WSPE, and NSPE, and is a registered professional engineer in the state of Wisconsin. Since 1949, he has published more than 300 research papers in the areas of microwaves and related electronics and has authored three books. He has five U.S. and foreign patents. In 1969, he received the T. C. Burnum IEEE Milwaukee Section Memorial Award for his contribution to microwave and millimeter-wave engineering and education. In 1984, he received the IEEE Centennial Medal Award for his extraordinary achievement in the same area. He received the ESM Engineer of The Year Award in 1988 in recognition of his distinguished service to the engineering profession.